Available online at www.sciencedirect.com

ScienceDirect

Energy Procedia 137 (2017) 460–467

Energy Procedia

www.elsevier.com/locate/procedia

14th Deep Sea Offshore Wind R&D Conference, EERA DeepWind'2017

Quasi-Static & Dynamic Numerical Modeling of Full Scale NREL 5MW Wind Turbine

M. Salman Siddiqui[a,b,*], Adil Rasheed[b], Trond Kvamsdal[a], Mandar Tabib[b]

[a]*Norwegian University of Science and Technology, Department of Mathematical Sciences, Alfred Getz vei 1, 7491 Trondheim, Norway*
[b]*CSE Group, Mathematics and Cybernetics, Sintef Digital, 7034, Trondheim, Norway*

Abstract

Simulations of the National Renewable Energy Laboratory (NREL) 5MW wind turbine under quasi-static Multiple Reference Frame (MRF) and dynamic Sliding Mesh Interface (SMI) methodologies are presented. Two reference zone approach is considered, inertial and moving reference frame. The former contains nacelle and tower, while the later constitutes of the rotor assembly. Predictive capabilities of both simulation techniques are exploited, and verification is performed against the Blade Element Momentum (BEM), and Large Eddy Simulation (LES) results in literature [1], [2]. The simulations are parametrized at variable tip-speed ratios (6, 6.5, 7, 7.5, 8, 8.5,9) and a uniform incoming velocity of $9m/s$ using unsteady Reynolds-Averaged Navier-Stokes (RANS). The MRF simulation techniques accuracy and robustness are exploited, hereafter key features at various operating conditions inside flow field are identified up to three radii (3R) distance. Aerodynamic torque in the dynamic SMI simulations is observed to oscillate and vary between 2,550 kN m and 2,650 kN m over a revolution. The wake evolution adjacent to the turbine is found to characterized by three massive vortices along with a central vortex which determined the dynamics of the wake. The three blade vortices interact with the central vortex and get dissipated at the 3R distance from the turbine. Immediately behind the tower, increased turbulent intensity levels are reported which gradually reduce after ≈1.5R distance both in the vertical and horizontal direction.

Peer-review under responsibility of SINTEF Energi AS.

Keywords: Wind Energy, NREL 5MW Wind Turbine, Sliding Mesh Interface, Multiple Reference Frame, Computational Fluid Dynamics

1. Introduction

Among different sources of renewable energy, the wind is considered a viable source for generating clean electricity [3]. Significant higher outputs and lower cost of energy from the wind makes it a rapidly growing renewable energy resource around the world. Now, wind energy community wants to exploit the opportunity to gain maximum yields from regions having a higher potential of wind energy [4]. Hence larger rotors are being developed, which can extract higher energy from the wind. However, increasing sizes of the wind machines impart significant challenge

* Corresponding author. Tel.: +47-48628035
E-mail address: muhammad.siddiqui@ntnu.no, muhammad.siddiqui@sintef.no

1876-6102
Peer-review under responsibility of SINTEF Energi AS.
10.1016/j.egypro.2017.10.370

concerning aerodynamic and structural aspects of blades [5]. Hence, good verifications methods are desired which can accurately predict the performance of such large wind turbines before they have been installed.

Various methods are presently available for the prediction ranging from simple analytical models to highly complex and time intensive experimental techniques. However, both approaches offer certain limitations i.e. restrictions regarding wind tunnel sizes to simple approximations implied in calculations of Blade Element Momentum (BEM) analysis. Recently, Computational Fluid Dynamics (CFD) have emerged a viable technique to resolve flow field around wind turbines [6]. There are many numerical methods available to determine flow field using CFD, the most used at industrial scale is Reynolds-averaged Navier-Stokes (RANS), which are a time-averaged solution and require turbulence models for the closure of governing equations [7], [8]. A more computationally expensive and accurate technique are the Large Eddy Simulation(LES), which explicitly resolve large-scale motion and model the small scales. Whereas, the most accurate but highly computational intensive is the Direct Numerical Simulation (DNS) [9], which resolve the complete spectrum of the flow field. However, even the modern supercomputers are not able to simulate this behavior for practical engineering related problems.

To perform high-fidelity simulation on NREL 5MW wind turbine in the present study RANS based methodology is employed. The flow field is simulated using Sliding Mesh Interface (SMI) and Multiple Reference Frame (MRF) techniques. Similar investigations are performed in past by Jonkhman *et al.* [2] Bazilevs *et al.* [1], [10], [11] and Sørensen *et al.* [12], [13], [14] to simulate the mega–watt size wind turbines. The present results are compared to the investigations of Jonkman *et al.* and Bazilevs *et al.* The goal of the study is to identify the predictive capabilities of both simulation methodologies; here after a parametric analysis is conducted at various operating conditions to analyze the wake evolution and aerodynamic characteristics. The results are presented in terms of aerodynamic torque obtained from the transient and steady state simulations. Distribution of wake evolution downstream is comprehended by plotting the contours of velocity magnitude at various stations. The behavior of turbulent fluctuations is explored by analyzing the wake structure downstream of full-machine in the vertical and horizontal directions.

2. Approach and methods

2.1. CAD model

The 5MW NREL turbine consists of three 63m long blades defined in terms of Delft University (DU) and National Advisory Committee for Aeronautics (NACA) cross-sectional profiles (DU21, DU25, DU30, DU35, DU40

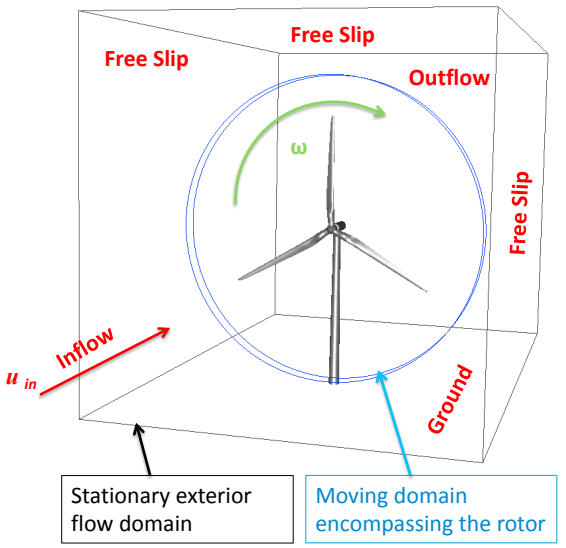

Fig. 1: NREL 5MW: Computational setup and boundary conditions of full problem domain. The extent of the domain is $4.75R \times 1.5R \times 3.2R$. Two zone approach is used with stationary and moving regions.

and NACA64) and twist angles at different locations away from the hub [15], [16]. The slight twist angle along the blade length helps in accommodating the variations in relative wind velocity from root to tip. The CAD model of full machine is shown in Figure 1.

2.2. Mesh

The mesh is generated in a way to allow hexahedral elements close to the turbine surface, and tetrahedral elements away from it. With highly dense mesh in the boundary layer, the non-dimensional wall distance to the first layers of nodes was kept up to the average $y^+ = 30$ [17]. This way a reduction in the computational cost is achieved with standard wall functions employed to model the characteristics of viscous sub-region and the buffer region. The mesh consists of approximately $10{\times}10^6$ cells and is shown in Figure 2.

2.3. Boundary conditions

In this study, CFD code OpenFOAM is employed which use certain acronyms for different boundary conditions. The inflow condition is specified in OpenFOAM as *Velocity inlet*, i.e. in our case the mean velocity was set to $(\overline{u}_x, \overline{u}_y, \overline{u}_z) = (9, 0, 0)$ m/s. The boundary condition at the downwind end of the computational fluid domain is specified as *Outflow*, i.e. zero pressure ($p = 0$). The upper, lower and side domain boundaries are specified as *Free-slip*, i.e. the velocity remains the same as of flow velocities beside the turbine. The two-zone approach is adopted; hence the rotor zone constitutes of turbine blades and hub which rotates during the transient simulations. Whereas, the stationary zone contains the turbine nacelle and the tower. The two zones are connected with the use of *Arbitary Mesh Interface* boundary condition [18].

2.4. Governing Equations

The governing Navier-Stokes equations are considered incompressible throughout the domain since the Mach number is always inside the limit of 0.3 in all simulations. The governing equations are solved in an inertial reference

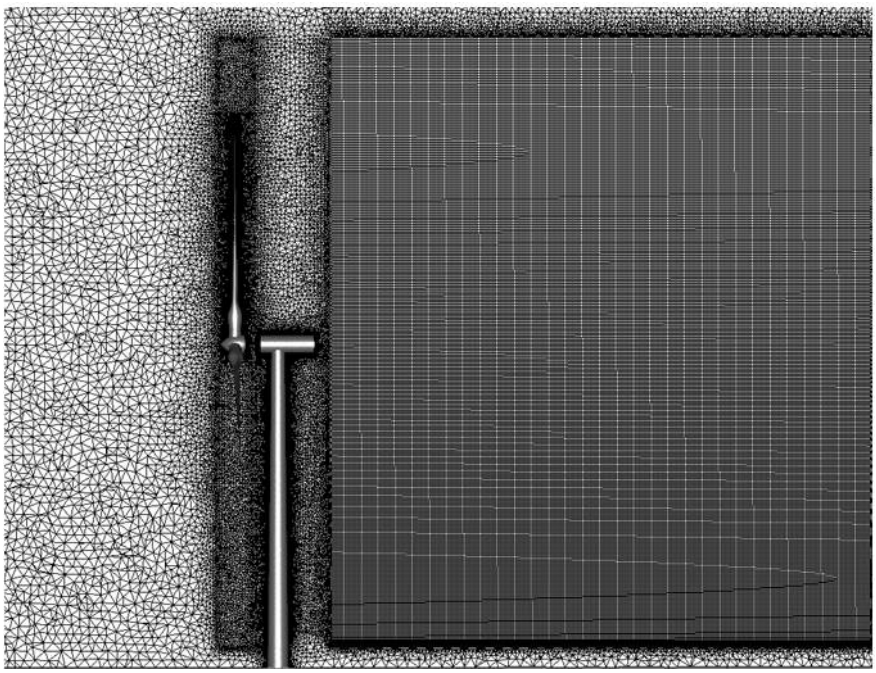

Fig. 2: NREL 5MW: Computational mesh consisting of hexahedral cells in the wake block and tetrahedral cells in the rest of domain. Prism extrusion is employed to allow finer mesh grading near the turbine surface. Mesh consist of $10{\times}10^6$ elements.

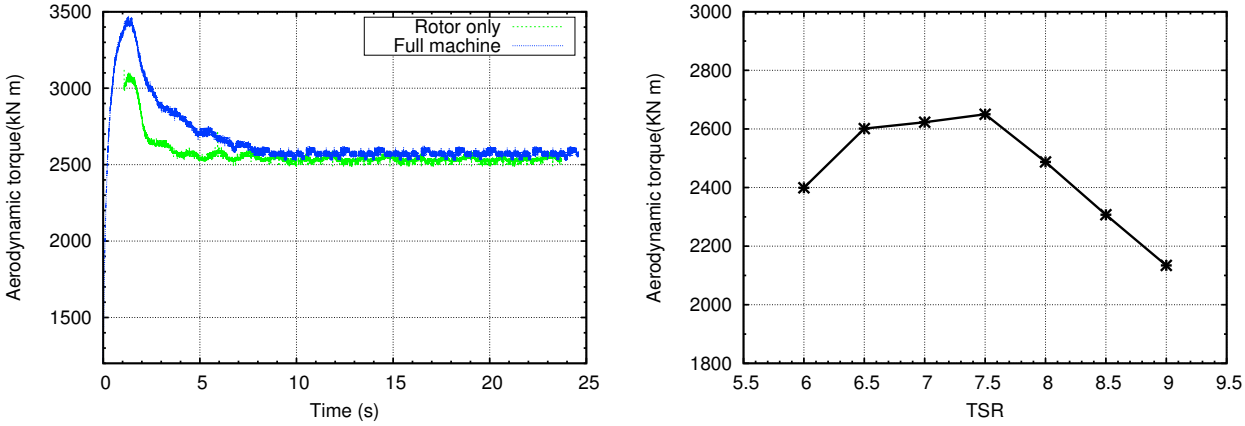

(a) NREL 5MW: Aeroydnmaic torque of SMI

(b) NREL 5MW: Aerodynamic torque of MRF at various TSR

Fig. 3: NREL 5MW: Time history of Aerodynamic torque. The dynamic evolution of torque over three rotation is plotted for SMI. Where as steady state torque values are plotted for different tip speed ratios using MRF.

frame with absolute velocity for the stationary zone of MRF constituting of turbine tower and nacelle. The following mass and momentum equations are solved:

$$\nabla \cdot \mathbf{u_a} = 0 \tag{1}$$

$$\nabla \cdot (\mathbf{u_a} \otimes \mathbf{u_a}) = -\nabla p + \nabla \cdot (\nu + \nu_t)\nabla(\mathbf{u_a} + (\nabla \mathbf{u_a})^{\mathbf{T}}) \tag{2}$$

where $\mathbf{u_a}$ is the absolute velocity as seen from a stationary reference frame.

To account for the affects of rotation inside the rotating zone, source terms are added in terms of Coriolis and centrifugal forces. The equations are written in terms of the relative flow velocity $\mathbf{u_r}$, which is a resultant vector arises from the velocity triangle of incoming and the induced velocity from the turbine blade.

$$\nabla \cdot \mathbf{u_r} = 0 \tag{3}$$

$$\nabla \cdot (\mathbf{u_r} \otimes \mathbf{u_r}) + \mathbf{2\Omega} \times \mathbf{u_R} + \mathbf{\Omega} \times (\mathbf{\Omega} \times \mathbf{r}) = -\nabla p + \nabla \cdot (\nu + \nu_t)\nabla(\mathbf{u_r} + (\nabla \mathbf{u_r})^{\mathbf{T}}) \tag{4}$$

$$\mathbf{u_a} = \mathbf{u_r} + \mathbf{\Omega} \times \mathbf{r} \tag{5}$$

where $\mathbf{\Omega}$ is the rotational speed of the reference frame with respect to a stationary observer (here it will also be equal to the rotational speed of the turbine), p is pressure, ν is the kinematic viscosity and ν_t is the turbulent kinetic viscosity.

In the SMI approach, the turbine rotates physically at each time step; hence it is no longer necessary to model the effects of rotation. The governing equations are solved now only in inertial reference frame and are as follows

$$\nabla \cdot \mathbf{u_a} = 0 \tag{6}$$

$$\frac{\partial \mathbf{u_a}}{\partial t} + \nabla \cdot (\mathbf{u_a} \otimes \mathbf{u_a}) = -\nabla p + \nabla \cdot (\nu + \nu_t)\nabla(\mathbf{u_a} + (\nabla \mathbf{u_a})^{\mathbf{T}}) \tag{7}$$

2.5. Solver settings

Second order accurate *Finite Volume Method (FVM)* spatial discretization is employed together with (explicit) *Forward Euler* time integration. The Reynolds number given by the relative flow velocity and the chord length at 75% blade location is calculated to be around 12×10^6 at the design tip speed ratio of 7.5. To model the effects of turbulence, $k - \omega$ SST model is chosen. For the base case used in [15], [2], reference fluid density $\rho = 1.225 kg/m^3$, dynamic viscosity $\mu = 1.82 \times 10^{-5} kg/m.s$ and incoming wind velocity $U_\infty = 9m/s$ and turbine rotational speed

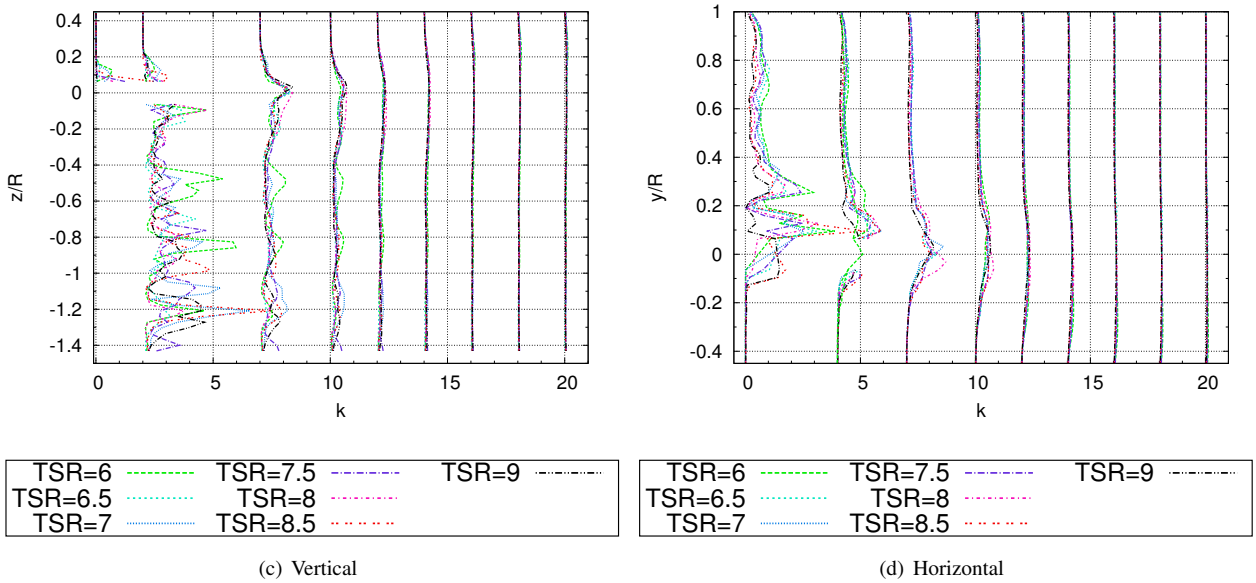

(c) Vertical (d) Horizontal

Fig. 4: NREL 5MW: Turbulent fluctuations downstream of turbine for different tip-speed-ratio and at different locations (0.15R, 0.30R, 0.45R, 0.60R, 0.90R, 1.30R from the hub). Note*: Successive profiles has been offset for better clarity

$\Omega = 10.313 rpm$ is used. Several more simulations are conducted with the same inlet velocity seven different tip speed ratios (TSR=6, 6.5, 7, 7.5, 8, 8.5, 9). A self-adjusting time step based on a maximum Courant number of 1 is used to keep the numerical accuracy of SMI simulations in range. The solver is created in OpenFOAM-2.3.0 (OF). To ensure continuity, OF uses an elliptic equation for the modified pressure which involves combining the continuity equation with the divergence of momentum equation. This elliptic equation along with the momentum equation and turbulence equation are solved in a segregated manner using the Semi-Implicit Method for Pressure-Linked Equations (SIMPLE) algorithm. The OF uses a finite volume discretization technique; wherein all the equations are integrated over control volumes (CV) using Green-Gauss divergence theorem. The Gauss divergence theorem converts the volume integral of the divergence of a variable into a surface integral of the variable over faces comprising the CV. Thus, the divergence term defining the convection terms can simply be computed using the face values of variables in the CV. The face values of variables are obtained from their neighboring cell centered values by using convective scheme. In this work, all the equations (except k and turbulence equations) use second order linear discretization scheme, while the turbulent equations use upwind convection schemes. Similarly, the diffusion term involving Laplacian operator (the divergence of the gradient) is simplified to compute the gradient of the variable at the face. The gradient term can be split into a contribution from the orthogonal and the non-orthogonal parts, and both these contributions are accounted for [19]. The SMI simulation at the TSR=7.55 is performed on 256 cores of a 2.6GHz Intel(R) Xeon(R) CPU machine on *Vilje*, the high-performance computational facility at Norwegian University of science and technology. They required almost one week to simulate one turbine rotation. However, the MRF simulations are run with 8 cores on a 3.2 GHz Intel(R) Xeon (R) CPU machine and converged in three days at a particular tip-speed.

3. Simulation results

This section outline results of computations performed on the NREL5 MW baseline wind turbine with two methodologies. The MRF methodology employed on 120^o rotor sector with cyclic boundary conditions were published in the literature before [19]. Herein we, perform the simulations on the full machine including the rotor (blades and hub), nacelle, and tower.

3.1. Torque characteristics

The Figure 3(a) contains the time history of the aerodynamic torque corresponding to full-machine and the rotor only simulations. The SMI torque history has shown highly irregular initial instabilities in the flow field which decayed after approximately two revolutions. Hereafter, the aerodynamic torque history started to settle towards the constant values. Oscillation around the mean values appeared due to the moving separation of flow from the blades during the rotation. This cause the aerodynamic coefficients to fluctuate about the mean value which ultimately causes the aerodynamic torque to vary intermittently. Hence, torque values are observed to oscillate around 2,550 kN m and 2,650 kN m over one rotation from the simulations. The values obtained are in close agreement with the 2670 kN m and 2500 kN m values published by Jonkhman *et al.* [2] and Bazilevs *et al.* [10], [11] respectively.

Whereas the steady torque values computed from the MRF method at the design TSR=7.55 is found to be slightly higher but in close agreement with the mean value obtained from SMI simulations. The smaller differences are mainly attributed to the inherent differences in the modeling characteristics of the two approaches. However, the simulation time for the MRF is significantly lower as compared to the SMI, hence a parametric analysis is conducted to evaluate the distribution of torque at the range of tip-speeds as shown in Figure 3(b). The torque obtained depict a bell shape curve, and the reason for low torque at lower and higher tip speeds is related to flow dynamics in the spanwise direction of blade [19]. It is found that at lower tip speeds, a significantly larger portion of the blade is operating under stall regime. Thus lower aerodynamic coefficients caused less contribution towards positive torque values. As the tip speed becomes higher and approaches 7.5, the angle of attack for most of the airfoil cross sections becomes optimal which cause maximum gains to the aerodynamic torque. Whereas with the further rise in the tip speed causes the angle to become lower and results in a smaller output of torque.

3.2. Wake characteristics

MRF methodology is employed to predict accurate assessment of overall aerodynamic behavior, thus the variation in wake characteristics are studied at variable operating conditions (6,6.5,7,7.5,8,8.5,9). First, the characteristics of the wake dynamics are investigated in terms of wake evolution behind the turbine at a particular tip-speed. Then the behavior of chaotic fluctuations behind the wind turbine is addressed over the range of operating conditions.

The contours of velocity magnitude at various stations downstream are plotted in Figure 5. It can be seen that the wake in the downstream direction is composed of rotating eddies emanating from each blade. To understand the initial flow field better adjacent to the rotor, streamlines of flow field are plotted across the turbine surface in the streamwise direction. It highlights certain important characteristic of flow evolution and its decay in the downstream direction. Most significant is the development of three large vortices corresponding to each turbine blade. Moreover, one large vortex is also formed near the central hub of the turbine. While convecting downwards, the central vortex interacts with the three counter-rotating vortices emanated from the blades. It causes the vortices to break down into smaller eddies before getting dissipated by the viscosity present inside the fluid [20].

On the other hand, turbine structure causes a significant increase in the turbulent intensity level inside the flow. Figure 4 depicts the characteristics of profiles over the range of tip-speeds at the various position downstream of the turbine. Turbulent fluctuations enhance wake recovery and promote turbulent diffusion. Hence a significant increase in the dissipation of vortices adjacent to the turbine is observed. The magnitude of turbulent fluctuations is found to be higher at higher tip speed ratio as compared to the lower ones. Whereas, an intermediate behavior of profiles at TSR 6 and 9 is observed at the design conditions of TSR=7.55. The magnitude of fluctuations is found to decay with distance away from the tower. A drop of almost 50% in fluctuations from the first station to the second is observed. At about 0.45R, fluctuations are found to settle down in the vertical direction. Whereas, in the horizontal direction, the fluctuations extracted at various stations are closer to each other over the range of operating conditions. The fluctuations are found to be asymmetric across the turbine center. It is believed to happen due to uneven flow distribution across the rotor. The turbine wake rotates in the opposite direction to the rotor and impart larger fluctuations on one side. Moreover, wake's strength varies in the downstream direction and is mainly dependent on operating turbine tip speed, therefore different peeks in the fluctuations are observed over the range of tip speed ratios. But most of the horizontal fluctuations begin to diffuse and settles down at around 3R distance away from the turbine. Hence the strength of vortices is lower at this station.

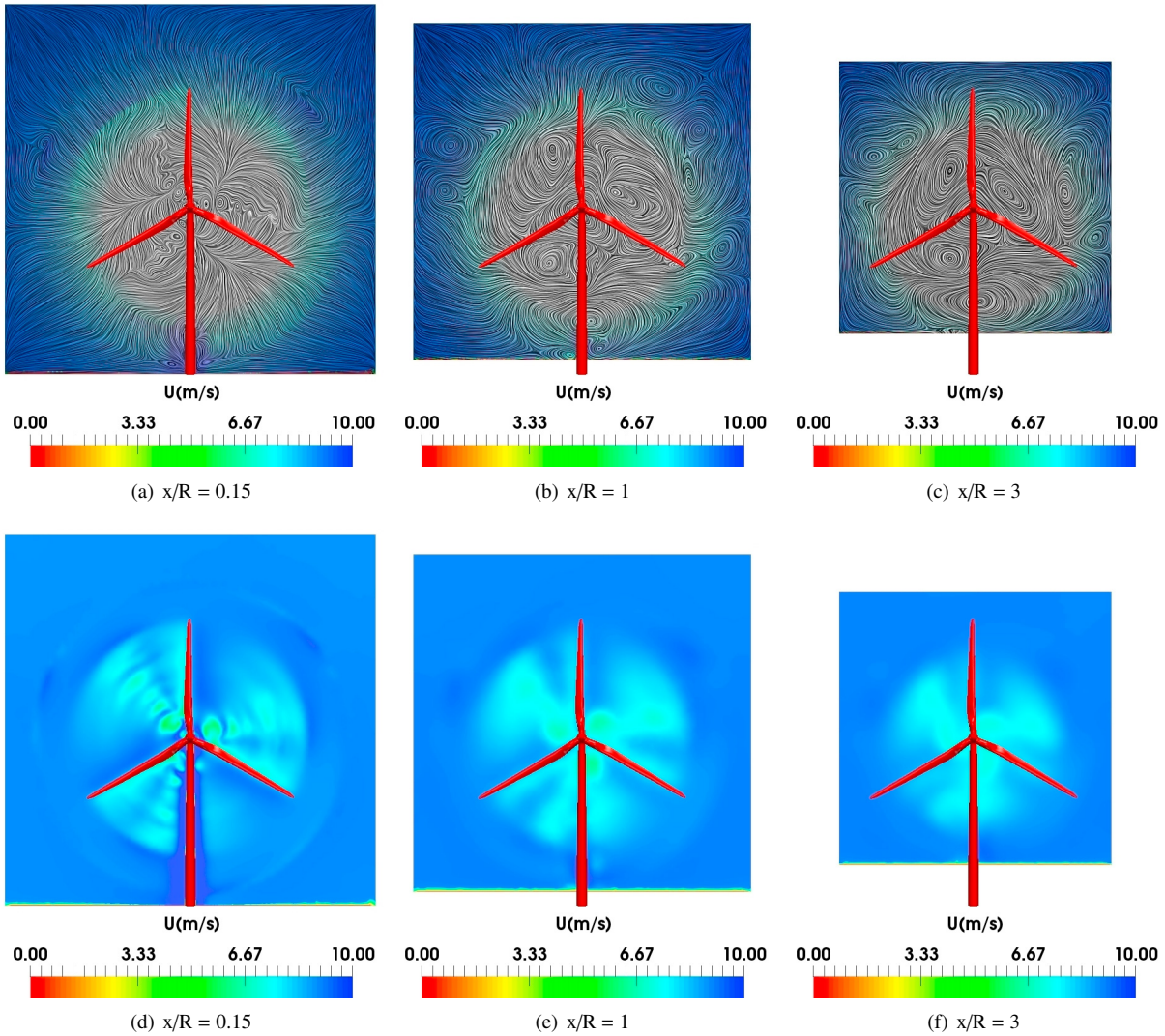

(a) x/R = 0.15 (b) x/R = 1 (c) x/R = 3

(d) x/R = 0.15 (e) x/R = 1 (f) x/R = 3

Fig. 5: NREL 5MW: Vorticity contours (top) and velocity magnitude (bottom) at three stations downstream of the domain (inertial reference frame). Significant vortices emanating from the turbine blade can be observed from the trailing edge. The velocity magnitude is restricted to 10m/s to provide better contrast.

4. Conclusion

An aerodynamics analysis of wind turbine with the quasi-static and dynamic behavior of NREL 5MW reference turbine was conducted constituting of full machine. Reynolds Average Navier Stokes (RANS) model was employed, and comparison of aerodynamic torque was performed with the available BEM and LES simulation results in the literature [2], [10]. Results presented have shown that Computational Fluid Dynamics (CFD) predictions match the test data consistently well. Since large wind turbines operate in time-varying conditions, first a Sliding Mesh Interface (SMI) analysis was conducted to analyze the turbine performance at the design tip speed ratio of 7.55. However, Multiple Reference Frame (MRF) seems to be a valuable approach combining accuracy and efficiency regarding aerodynamic modeling of wind machines under various operating conditions. Torque contribution was observed to vary from 2,550 kN m to 2,650 kN m for transient analysis. Snapshots of velocity contours have predicted the evolution of three dominant vortices emanating from each blade, which interact with the central vortex and break down into smaller eddies before getting dissipated. Increased levels of turbulent intensity were found close to the hub

where velocity gradients are higher as compared to the outer region which showed significantly fewer gradients. Due to high molecular diffusion and dissipation effects, turbulent fluctuations started to settle down away from the turbine. Therefore small values of turbulent intensity were observed approximately around 3R of the turbine.

Acknowledgments

The authors acknowledge the financial support from the Norwegian Research Council and the industrial partners of NOWITECH: Norwegian Research Centre for Offshore Wind Technology (Grant No.:193823/S60) (www.nowitech.no) and FSI-WT (Grant No.:216465/E20)(http://www.fsi-wt.no). The authors greatly acknowledge the Norwegian meta-center for computational science (NOTUR-reference number: NN9322K/1589)(www.notur.no) for giving us access to the Vilje high-performance computer at the Norwegian University of Science and Technology (NTNU).

References

[1] Bazilevs, Y., Hsu, M., Kiendl, J., Benson, D.. A computational procedure for prebending of wind turbine blades. International Journal for Numerical Methods in Engineering 2012;89(3):323–336.
[2] Jonkman, J., Marshal, L., Buhl, J.. FAST users guide, National Renewable Energy Laboratory, Golden, CO, Tech. Rep. NREL/TP-500e38060. 2005.
[3] Siddiqui, M.S., Durrani, N., Akhtar, I.. Quantification of the effects of geometric approximations on the performance of a vertical axis wind turbine. Renewable Energy 2015;74(0):661–670.
[4] Siddiqui, M.S., Durrani, N., Akhtar, I.. Numerical study to quantify the effects of struts and central hub on the performance of a three dimensional vertical axis wind turbine using sliding mesh. ASME Power Conference 2013;2(POWER2013-98300):V002T09A020(11).
[5] Siddiqui, M.S., Rasheed, A., Tabib, M., Kvamsdal, T.. Numerical Modeling Framework for Wind Turbine Analysis and Atmospheric Boundary Layer Interaction. AIAA SciTech Forum; American Institute of Aeronautics and Astronautics; 2017,Doi:10.2514/6.2017-1162.
[6] Siddiqui, M.S., Rasheed, A., Kvamsdal, T., Tabib, M.. Effect of turbulence intensity on the performance of an offshore vertical axis wind turbine. Energy Procedia 2015;80:312–320.
[7] Nordanger, K., Holdahl, R., Kvarving, A.M., Rasheed, A., Kvamsdal, T.. Implementation and comparison of three isogeometric Navier-Stokes solvers applied to simulation of flow past a fixed 2D NACA0012 airfoil at high Reynolds number. Computer Methods in Applied Mechanics and Engineering 2015;284:664–688.
[8] Nordanger, K., Holdahl, R., Kvamsdal, T., Kvarving, A.M., Rasheed, A.. Simulation of airflow past a 2D NACA0015 airfoil using an isogeometric incompressible Navier-Stokes solver with the Spalart-Allmaras turbulence model. Computer Methods in Applied Mechanics and Engineering 2015;290:183 – 208.
[9] Bazilevs, Y., Hsu, M.C., Akkerman, I., Wright, S., Takizawa, K., Henicke, B., et al. 3D simulation of wind turbine rotors at full scale. part *I*: Geometry modeling and aerodynamics. International Journal for Numerical Methods in Fluids 2011;65(1-3):207–235.
[10] Hsu, M.C., Bazilevs, Y.. Fluid–structure interaction modeling of wind turbines: simulating the full machine. Computational Mechanics 2012;50(6):821–833.
[11] Hsu, M.C., Akkerman, I., Bazilevs, Y.. Finite element simulation of wind turbine aerodynamics: Validation study using NREL Phase VI experiment. Wind Energy 2014;17(3):461–481.
[12] Heinz, J.C., Sørensen, N.N., Zahle, F.. Fluid-structure interaction computations for geometrically resolved rotor simulations using CFD. Wind Energy 2016;19(12):22052221.
[13] Cavar, D., Rthor, P.E., Bechmann, A., Sørensen, N., Martinez, B., Zahle, F., et al. Comparison of OpenFOAM and Ellipsys3D for neutral atmospheric flow over complex terrain. Wind Energy Science Discussions 2016;1:55–70.
[14] Guntur, S., Sørensen, N.N., Schreck, S., Bergami, L.. Modeling dynamic stall on wind turbine blades under rotationally augmented flow fields. Wind Energy 2016;19(3):383397.
[15] Jonkman, J.M., Butterfield, S., Musial, W., Scott, G.. National Renewable Energy Laboratory. 2009.
[16] Kooijman, H.J.T., Lindenburg, C., Winkelaar, D., Hooft, E.L.V.D.. DOWEC 6 MW pre-design: Aero-elastic modeling of the DOWEC 6 MW pre-design in PHATAS, Dutch Offshore Wind Energy Converter 1997-2003 Public Rceports , DOWEC 10046-009, ECN-CX–01-135, Petten, the Netherlands. 2003.
[17] Wilcox, D.. Simulation of transition with a two-equation turbulence model. AIAA Journal 1994;32:247–255.
[18] Jasak, H.. Dynamic mesh handling in openfoam. 47th AIAA Aerospace Sciences Meeting 5-8 January, 2008;52:(AIAA 2009–341).
[19] Siddiqui, M.S., Rasheed, A., Tabib, M., Kvamsdal, T.. Numerical analysis of NREL 5MW wind turbine: A study towards a better understanding of wake characteristic and torque generation mechanism. Journal of Physics: Conference Series 2016;753(3):032059.
[20] Salehyar, S., Zhu, Q.. Aerodynamic dissipation effects on the rotating blades of floating wind turbines. Renewable Energy 2015;78(0):119–127.